08

Electric potential of micro-sized blocks at the $NaNbO_3$ film surface

© *M.A. Bunin, V.A. Yorshin, K.S. Chumachenko, I.P. Raevskii*

Southern Federal University, Research institute of Physics, Rostov-on-Don, Russia
e-mail: bunin.m.a@gmail.com

Received December 4, 2024
Revised February 14, 2025
Accepted February 17, 2025

The properties of the inherent electric potential of a $\sim 0.1\,\mu m^2$ — size blocks at the $NaNbO_3$ film surface grown under conditions of unstable misfit strain are analyzed. The results are applied in a qualitative model of injected charge dissipation taking into account the potential of these blocks

Keywords: sodium niobate, thin film, surface, electric potential, electric charge, misfit strain, electret.

DOI: 10.61011/TP.2025.06.61382.436-24

Introduction

Improving the reliability and performance of non-volatile memory devices requires a deep understanding of charge injection/generation, transport, localization and storage mechanisms [1]. Special attention is paid to nanoscale ferroelectric (FE) materials — films. The methods their characteristics are formed is called a „deformation engineering“ [2]. They exploit the misfit strain (MS) at the film/substrate interface to control the film material properties. The latter may differ significantly from the properties of the crystal and from a film of the same composition on another substrate [3–6].

Previously, an epitaxial [001]-oriented $NaNbO_3/SrRuO_3/MgO$(NNO) heterostructure with a thickness of 500 nm was obtained, the ferroelectric properties of which are due to the misfit strain [7,8]. The morphology and dissipation of the injected charge on its surface, formed by co-directional blocks of size$\sim (0.8-1.1)\times(0.1-0.3)\,\mu$m and height $\sim 20-40$ nm (up to 50 nm), were studied using scanning probe microscopy (SPM). In [10] it is shown that unstable MS is possible in it, creating an electret-like state of surface blocks. Their small inherent electric potential ($\sim(-(15-25))$ mV) is clearly visible before charge injection (Fig. 1, *a, b*). It changes over time otherwise than for injected areas (Fig. 1, *h*) (see Sect.2 below).

The stability of the electret state depends on the external field and on the field of the externally injected charge [11–15]. Its relaxation goes through two stages: after rapid dissipation, the sign of the field inverts and the stage of its slow attenuation begins [12,13]. The reason is considered to be the mutual influence of two self-consistent processes: the misorientation of dipoles and the neutralization of the internal electric field due to the electrical conductivity of the sample [12]. As a result, the relaxation time of the electret state is significantly increased. However, until now only weak electret properties of sodium niobate ceramics are known [16]; for films, such data are not yet available.

It is known that initial state of the FE surface may significantly influence the charge dissipation [17]. It can be significantly influenced by the electret nature of the electric potential of the blocks, in particular, when it is inverted. Therefore, studying the features of the change in surface potential during dissipation will allow us to check the electret nature of the properties of blocks on the surface of the NNO film and take it into account in a qualitative model of dissipation of the injected charge.

1. Experimental conditions and models for describing the MS properties

In order to take into account the dissipation of charges that differ significantly in magnitude (intrinsic which are inherent in the surface blocks and externally injected), it is necessary to ensure that under the experimental conditions in [9] there are no pecularites that interfere with this. It is also desirable that the model describing the characteristics of the film, including the surface potential, correspond to its properties.

1.1. SPM experiment

The results of SPM measurements of ferroelectric films can be affected by local polarization screening, polarization reversal, surface screening, probe pressure on the surface, and unexpected back switching (this was discussed in details in the work [17]). We will briefly discuss this below. These processes are known to require quite high level of voltage on the probe ($\gtrsim(4-13)$ V) ([17] and references in it), that were not used in our work [9] (see below, Section 2). Switching is possible under high pressure of the probe on the surface. In [9], it is small: the force $\sim 2\cdot 10^2$ nN is not enough to noticeably change the electrical potentials of the blocks or cause the discharge of pre-existing surface charges (if any). This is confirmed by the absence of electrical potential in the area corresponding to the tip bias 0 V [9]. In general, the experimental conditions in work [9] ensure

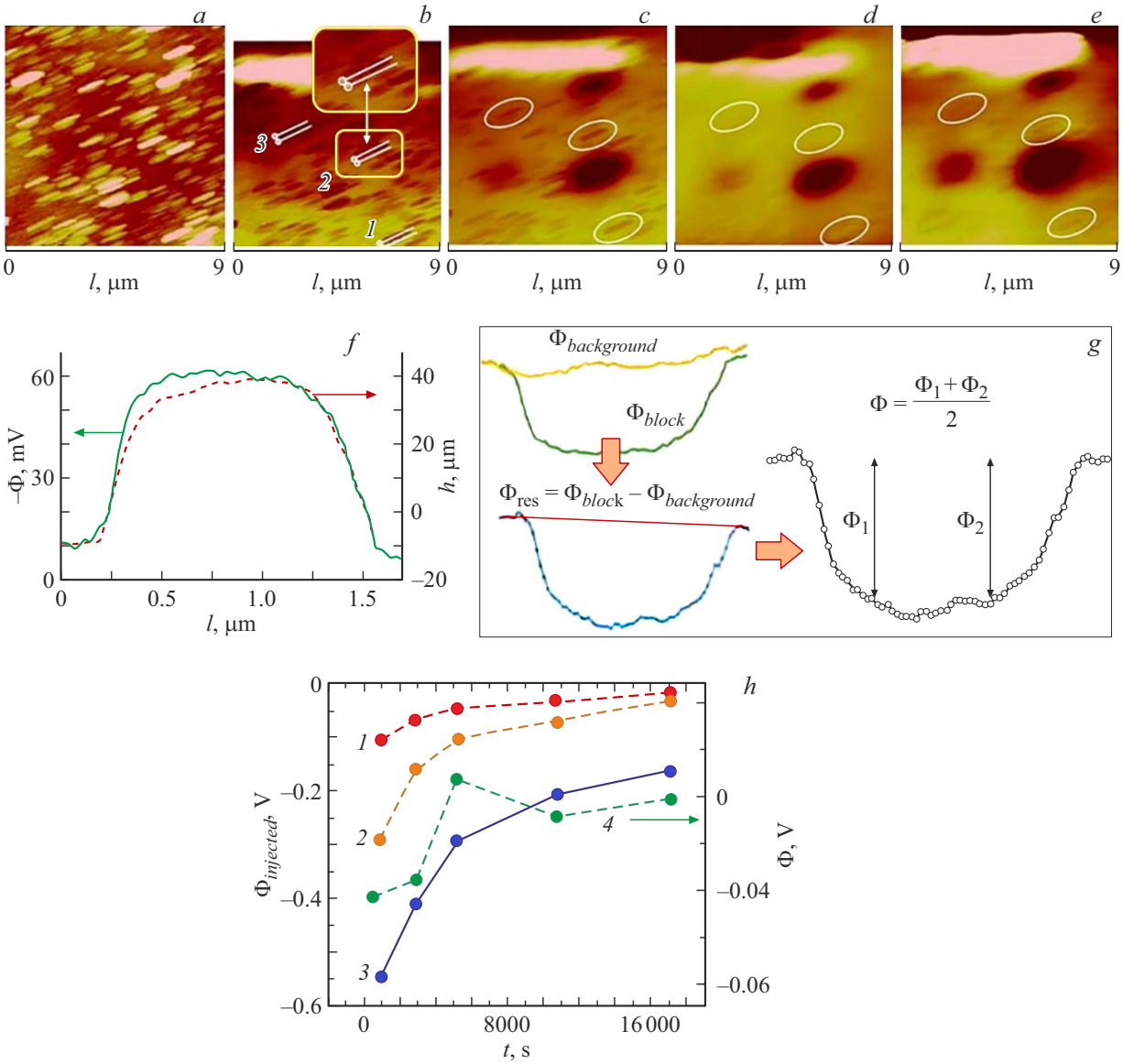

Figure 1. Images of relief and electric potential of the $NaNbO_3$ film surface (the data are taken from [9]). *a* — relief; *b–e* — electrical potential: *b* — before the charge injection (three typical blocks are designated by numbers 1, 2, 3; the background level are taken along white lines traced close to the block); *c* — through ~ 3000 s; *d* — through ~ 5000 s; *e* — through ~ 17 000 s. *c–e* -The contrast of the images has been increased to make subtle details more visible; white ovals indicate the locations of the *1–3* blocks in the figure *b*; *f* — cross-sections of the block relief and its electric potential (example in the image relates to the block № 2 (*b*)); *g* — scheme for calculating the electrical potential of surface blocks: $\Phi_{background}$ — electric potential of the background, Φ_{block} — electric potential of the block, Φ_{res} — electric potential of the block after background subtraction, its values Φ_1 and Φ_2 are taken at a distance of~ 1/4 from the left and right edges of the block, respectively; *h* — electric potentials versus time dependencies: *1–3* — for injected areas at tip bias values −1, −2, and −3 V respectively; *4* — for the surface blocks. Connecting lines are drawn for ease of perception. The method of selecting the profile of the surface cross-section is shown in *b, g*.

that there are no feasible distortions of the measurement results due to the reasons discussed in [17].

1.2. Models for describing the properties of MS in films

The principles of the phenomenological modeling of the interface properties in thin ferroelectric films were considered in the works of Glinchuk et al. [18,19] and Tagantsev et al. [18]. These approaches differ, among other things, in their understanding of the role of MS in the formation of film properties and the reasons for the origin of its characteristics. Comparison of these approaches will allow us a reasonable estimation of the NNO film properties.

In the [18–21] models, the source of the field constituted at the interface is the mechanical coupling between the ferroelectric and the substrate. However, in the models of works [18,19] and [20,21] the sequence of reasons of

its occurrence is considered differently. In [18,19] the combination of the misfit between the lattice parameters of the film and the substrate and the piezoelectric effect (a d_{31} coefficient) creates an electric field, which magnitude estimation for the PZT 50/50 film gave quite reasonable agreement with the experimental data. The initial assumptions take into account the temperature dependence of MS.[1] In [10] the characteristics of NNO film were estimated according to the model [18,19]. The obtained values made it possible to explain the measurement results in [7] and to assume the possibility of the existence of an electret-like state for the surface blocks of the NNO film in [10].

In works [20,21], models of interface-induced phenomena affecting the switching characteristics and dielectric properties of thin ferroelectric films were considered. It was assumed that deformation at the interface leads to the appearance of misfit dislocations (MDsl) on it, which are localized in a small vicinity near it (no more than a few monolayers). While moving away from the border, the strain decreasing, creating a deformation gradient that causes linear polarization due to the flexoelectricity (FlE) and stimulates the release of dislocation stresses. Due to FlE, an electric field is created, and its out-of-plane component creates polarization [20,21]. With that, the authors warn that the sizes of the objects they are considering may be close to the border of suitability of the continuum approach. The temperature dependence of the MS was not taken into account, and this dependence itself was used only as a parameter for assessing the boundary of the influence of MDsl. Recent studies of [22–24] have shown a different situation: for example, in a material with a large lattice misfit, dislocations appear mainly at a certain distance from the interface (~ 6 nm in [19], up to ~ 100 nm in [24]). Therefore, in our case this approach is less preferable, especially since the thickness of the NNO film under study is significantly greater than those considered in [20,21].

In general, the conditions of the surface electric potential measurements in [9] do not indicate that there's a significant impact from the effects that could distort or influence the measurement results. The approach to describing the properties of NNO surface blocks proposed in the model [18,19] gives results that agree with experiment. This allows the analysis of low contributions to the surface potential when considering the dissipation of the injected charge.

2. Results and discussion

In [9] the charge was injected by SPM probe in regions $(0.5 \times 0.5)\,\mu$m; the tip bias values were: 0, -1, -2 and -3 V under constant experimental conditions. In Fig. 1, $b-e$ changes in the scan images of the surface blocks electric potential during the measurements are shown. First, we discuss the morphological features of the surface potential, and then the charge dissipation.

The possibility of non-stationary MS in obtaining NNO films is shown in [10]. Its manifestation is possible both in the transverse and lateral directions relative to the interface. In the first case, due to the difference in lattice parameters, the lower layer acts as a substrate for the upper one. The lateral MS forms a lateral anisotropic deformation in the epitaxial film. As a result, areas of heterogeneity with a deformation gradient appear, which creates heterogeneity in the properties of surface blocks. This is consistent with the results of [25,26], where MS forms a lateral anisotropic deformation that depends on the thickness, lattice parameters, and thermal expansion coefficient of the epitaxial film. It is also known that in polycrystalline ceramics, the strong anisotropy of thermal expansion creates mechanical stresses [27]. This description is quite consistent with the results of SPM measurements in Fig. 1: on the scans of the electric potential there are blocks with positive or close to zero potential values, which appear lighter than others in the image. At the same time, in the histograms of the distribution of the surface electric potential in [9], negative values predominate, which explains the unipolarity of the film observed in [7].

Let us consider a qualitative description of the influence of the electret state of surface blocks on the dissipation of the injected charge.

The cross-section profiles of the relief and potential of the surface block in Fig. 1 have a rectangular-like shape with a ratio of the axis lengths $\sim 1/(4-5)$. This is $\sim (1.8-2.5)$ times larger than for the elliptical spots of injected potentials in [9], and may indicate different charge dissipation mechanisms for the surface blocks and for the injected regions. Comparison of the dependencies in Fig. 1, h confirms this: injected regions — curves *1–3*; blocks — curve *4*.

The shape of the electric potential spots from the injected charges is an ellipse with the axial ratio $a/b \sim (1.8-2.8)$ (their morphology is described in detail in [9]). This value depends on the time and on the tip bias during injection (Fig. 2). For the tip bias -3 V and -2 V the dependencies are generally similar. The highest value of $a/b = 2.8$ is achieved in the same time interval in which the electric potential of the surface blocks in Fig. 1, h (~ 5100 s) changes its sign (inversion). For the tip bias -1 V the ratio $a/b \sim (1.8-2.0)$.

According to the principles of crystallography, the value of a/b is determined by the mutual orientation of the surface of the epitaxial film and the principal axes of its conductivity tensor, the directions of which depend on the space group describing the phase state. If the orientations do not correspond to each other, then the ratio a/b depends on the linear combination of the corresponding projections.

[1] Most often, the material parameters allow ignoring the temperature dependence of MS. There's a different story for sodium niobate [10].

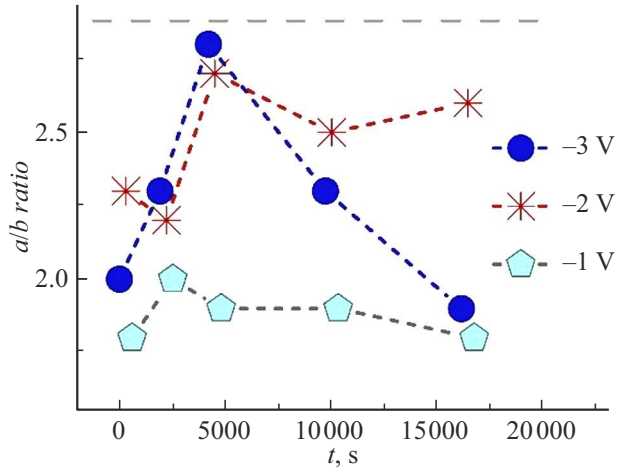

Figure 2. Change of a/b ratio over time for spots of electric potential of the injected charge at different tip biases. Connecting lines are drawn for ease of perception. The horizontal dashed line corresponds to „ideal" value of $a/b = 2.88$ calculated for the r-phase of $NaNbO_3$.

In the work [18,19] it was established that the electret-like state is formed from the r-phase[2] of the film surface material. Thus, assuming that according to [28], $a/b = (\varepsilon_x/\varepsilon_y)^{1/2}$, from the data for the$r$- phase of NNO in [29,30], we obtain: $a/b = 2.88$ (dashed line in Fig. 2) which is close to the highest value 2.8. This is achieved in the time interval corresponding to the inversion of the electrical potential of the blocks (Fig. 1, h).

Let's qualitatively describe the dependences a/b in Fig. 2. We assume that the effective field $\mathbf{E}$ acting on the charge carriers is formed by the contributions $\mathbf{E}_{inj}$ of the injected charge field, $\mathbf{E}_{elt}$ of the electret charge field of the blocks and (if present) by the $\mathbf{E}_{ext}$ of the external charge field (in Fig. 1, b–e - a large spot of positive charge is observed in the upper part of the scans; see also [9]):

$$\mathbf{E} = \mathbf{E}_{inj} + \mathbf{E}_{elt} + \mathbf{E}_{ext}, \qquad (1a)$$

$$\mathbf{E}_{inj} = \mathbf{E}_{crst} + \mathbf{E}_S. \qquad (1b)$$

The field $\mathbf{E}_{inj}$ of injected charge consists of two components: $\mathbf{E}_{crst}$ — lateral („crystallographic" contribution) and $\mathbf{E}_S$ — normal (that causes leakage into the substrate). In pure form, $\mathbf{E}_{crst}$ can appear when other contributions to (1a) cancel each other or are negligible.

$\mathbf{E}_{elt}$ — field induced by the electret state of surface blocks. During inversion and transition to the slow relaxation stage, the sign of this field changes (Fig. 1, h). This occurs at $t \sim (5000–5100)$ s, when $a/b = 2.8$ value is maximum, which estimates the Maxwellian relaxation time of the electret state in the NNO. film. The sophisticated lateral distribution of the electric potential over the surface of film [9], due to unstable MS [10], does not allow us to obtain the values of $\mathbf{E}_{elt}$ from the estimate in [10] for field inducing the electret state. Moreover, the lateral components of the field in the thin-film electrets are negligible, and due to high surface resistance, it do not support the charge spreading [31]. Therefore, it is believed that the electret charge field is mainly directed normal to the surface.

$\mathbf{E}_{ext}$ — external charge field. It defines by the charge presence in the vicinity (e.g., see the upper part of the electric potential images in Fig. 1, b–e).

The total leakage into the substrate are found by the sum $\mathbf{E}_S + \mathbf{E}_{elt}$ (we assume that lateral leakage from the small charges of the blocks is negligible). At the beginning, at high injected charge density, $\mathbf{E}_S$ is predominate and $\mathbf{E}_S > \mathbf{E}_{elt}$. Over the time $\mathbf{E}_S$ declines and the contributions $\mathbf{E}_S$ and $\mathbf{E}_{crst}$ are become comparable. If the leakage into the substrate is low or absent (for example, for a thick film), the electret field of blocks $\mathbf{E}_{elt}$ can exceed $\mathbf{E}_S$.

When analyzing the a/b dependencies in Fig. 2, three variants are possible: a large field $\mathbf{E}_{inj}$ (tip bias is -3 V); injection in the presence of positive electric potential (for the spot created at -2 V bias); and a weak field (-1 V).

For the tip bias -3 V the injected charge is the largest, and $\mathbf{E}_{elt} \ll \mathbf{E}_S$ (about ~ 10 times at initial stage, Fig. 1, h). Over time, the density of the injected charge decreases, as well as $\mathbf{E}_{crst}$ and $\mathbf{E}_S$. Since the film thickness of 500 nm is significantly smaller than the distances between the injection areas ($> 5–7\,\mu$m), the leakage into the substrate prevails and $\mathbf{E}_S$ decreases faster than $\mathbf{E}_{crst}$, which relative contribution increases. This case, the ratio a/b increases which corresponds to Fig. 2. By the time of $t \sim (5000–5100)$ s the contribution $\mathbf{E}_S$ becomes comparable with $\mathbf{E}_{elt}$, which at this stage is inverted with change of sign (Fig. 1, h). Then mutual compensation of $\mathbf{E}_{elt}$ and $\mathbf{E}_S$ becomes possible, when the contribution $\mathbf{E}_{crst}$ remains almost the only one, and $a/b = 2.8$ is the largest. Subsequently, the density of the injected charge decreases due to leakage into the substrate. Herewith, the contribution from the electret blocks remains practically unchanged, and, consequently, the relative contribution of lateral leakage becomes greater. In this case, the ratio a/b gradually decreases, reaching the value ~ 1.9 at the end of the measurements. The value $\mathbf{E}_{elt}$ corresponds to the slow relaxation stage when the electret external field is low.

The possibility of the external charge field influence on dissipation is confirmed by the analysis of the spot created at the tip bias of -2 V. At a distance of $\sim 2\,\mu$m from it (~ 4 of typical size of the injected area) there is a region with a positive potential (see the upper part of the scan images in Fig. 1, b–e). At initial stage, up to ~ 5100 s, the dependencies at biases -2 V and -3 V are similar, however, after ~ 8000 s their dependencies are different. Beginning from ~ 10000 s, for bias -2 V the value a/b is $\sim (2.4–2.6)$ while for bias -3 V the a/b decreases from ~ 2.4 to $\sim (1.9–1.8)$ (Fig. 2). Apparently, the field of the positive charge reduces leakage into the substrate and lateral spreading. Its effect is limited to the nearest area only, it has

[2] The designation of the phase state of the film corresponds to that used in [18,19].

(almost) no effect on the spots for -3 V and -1 V biases, located at a distances of $\sim (1.5-2)$ times larger.

At the bias -1 V the injected charge is small, therefore, the relative contributions $\mathbf{E}_S$, $\mathbf{E}_{crst}$ and $\mathbf{E}_{elt}$ are comparable. Further, the dependence in part is similar to that observed for -3 V and -2 V, while the value of a/b slightly increasing, reaching ≈ 2.0 in the interval $\sim (2800-5000)$ s. After this, a/b decrease to $\sim (1.6-1.7)$ in the end of measurements.

Generally, the qualitative model described above allows us to explain the experimentally observed a/b dependences of the injected charge dissipation and to take into account the electret nature of the surface blocks electric potential. By varying the bias on the probe during injection and the distance to the adjacent charge region, the relaxation time and the resultant charge dissipation can be controlled.

Conclusions

The qualitative model of injected charge dissipation is consistent with the assumption of the electret origin of the electric field of the blocks on the surface of the [001]-oriented $NaNbO_3/SrRuO_3/MgO$ heterostructure. The maximum ratio of axes a/b of the elliptical spots of the injected charge electric potential (2.8) is close to that calculated from the crystallographic data for the r-phase of sodium niobate (2.88). When the surface charge dissipates, its value changes: it is greatest in the time interval when the electret potential of the surface blocks inverts. The charge dissipation is influenced by the charge located close ($\sim 2\mu$m) to the injected region, while more distant regions have virtually no effect. By varying the magnitude of the probe bias during injection and the distance to the adjacent charge region, it is possible to control the charge relaxation time in the injected region and the result of charge dissipation.

Funding

This study was supported financially by the Ministry of Education and Science of the Russian Federation (state research assignment for 2023, project № FENW-2023-0015).

Acknowledgments

Authors contribution: M.A. Bunin — concepts of work, experiment, models, discussion, text; V.A. Yorshin — obtaining and processing SPM experimental data; K.S. Chumachenko — processing SPM experimental data, discussion, graphic design; I.P. Rayevskii — discussion of the main concepts and results.

Conflict of interest

The authors declare that they have no conflict of interest.

References

[1] T. Mikolajick, S. Slesazeck, H. Mulaosmanovic, M.H. Park, S. Fichtner, P.D. Lomenzo, M. Hoffmann, U. Schroeder. J. Appl. Phys., **129**, 100901 (2021). DOI: 10.1063/5.0037617

[2] A.R. Damodaran, J.C. Agar, S. Pandya. J. Phys.: Condens. Matter., **28**, 263001 (2016). DOI: 10.1088/0953-8984/28/26/263001

[3] Y. Shiratori, A. Magrez, J. Dornseiffer, F.-H. Haegel, C. Pithan, R. Waser. J. Phys. Chem. B, **109**, 20122 (2005). DOI: 10.1021/jp052974p

[4] T.M. Shaw, S. Trolier-McKinstry, P.C. McIntyre. Annu. Rev. Mater. Sci., **30**, 263 (2000). DOI: 10.1146/annurev.matsci.30.1.263

[5] H. Liu, H. Wu, Kh.Ph. Ong, T. Yang, P. Yang, P.K. Das, X. Chi, Y. Zhang, C. Diao, W.K.A. Wong, E.P. Chew, Y.F. Chen, Ch.K.I. Tan, A. Rusydi, M.B.H. Breese, D.J. Singh, L.-Q. Chen, S.J. Pennycook, K. Yao. Science, **369**, 292 (2020). DOI: 10.1126/science.abb3209

[6] S.B. Anooz, Y.Wang, P. Petrik, M.de Oliveira Guimaraes, M. Schmidbauer, J. Schwarzkopf. Appl. Phys. Lett., **120**, 202901 (2022). DOI: 10.1063/5.0087959

[7] A.V. Pavlenko, D.V. Stryukov, N.V. Ter-Oganessian, Tech. Phys. Lett., 46, 62 (2020). DOI: 0.1134/S1063785020010289. DOI: 10.21883/PJTF.2020.02.48946.18063.

[8] A.V. Pavlenko, D.V. Stryukov, M.V. Vladimirov, A.E. Ganzha, S.A. Udovenko, A. Joseph, J. Sunil, Ch. Narayana, R.G. Burkovsky, I.P. Raevski, N.V. Ter-Oganessian. arXiv:2112.04579v1[cond-mat.mtrl-sci] 8 Dec 2021.

[9] M.A. Bunin, V.A. Yorshin, M.D. Miruschenko, I.A. Donchenko, A.V. Pavlenko, O.A. Bunina, I.P. Raevski. Ferroelectrics, **590** (1), 190 (2022). DOI: 10.1080/00150193.2022.2037950

[10] M.A. Bunin, I.P. Raevskii, Tech.Phys. Lett., 51, 58 (2025). DOI: 10.61011/TPL.2025.01.60140.20026 (2025). DOI: 10.61011/PJTF.2025.02.59548.20026

[11] G.M. Sessler. *Physical principles of electrets*. In G.M. Sessler (ed). *Electrets. Topics in Applied Physics* (Springer, Berlin, Heidelberg, 1980), v. 33, p. 13–80. DOI: 10.1007/3540173358_10

[12] Yu.A. Gorokhvatsky, G.A. Bordovsky. *Termoaktivatsionnaya tokovaya spektroscopia vysokoomnykh poluprovodnikov i dielektriko (Thermally activated current spectroscopy of high-resistance semiconductors and dielectrics)* (Nauka, M., 1991) (in Russian)

[13] F.T. Xu, S.M. Thaler, C.A. Lopez, J.A. Barnard, A. Butera, J.L. Weston. Appl. Phys. Lett., **86**, 074105 (2005). DOI: 10.1063/1.1868067

[14] A.N. Pavlov, Yu.A. Trusov, E.M. Panchenko, F.I. Savenko, V.P. Sakhnenko. J. Phys. D: Appl. Phys., **25** 1243 (1992). DOI: 10.1088/0022-3727/25/8/015

[15] H. Amjadi, C. Thielemann. IEEE Trans. Dielectr. Electr. Insul., **3**, 494 (1996). DOI: 10.1109/94.536727

[16] S.O. Lisitsina, E.M. Panchenko, I.P. Raevskii, Yu.A. Trusov, E.G. Fesenko. J. Electrostat., **24**, 295 (1990). DOI: 10.1016/0304-3886(90)90016-o

[17] S.V. Kalinin, Yu. Kim, D.D. Fong, A.N. Morozovska. Rep. Prog. Phys., **81**, 036502 (2018). DOI: 10.1088/1361-6633/aa915a

[18] M.D. Glinchuk, A.N. Morozovska, E.A. Eliseev. Ferroelectrics, **335**, 257 (2006). DOI: 10.1080/00150190600691593

[19] M.D. Glinchuk, A.N. Morozovska, E.A. Eliseev. J. Appl. Phys., **99**, 114102 (2006). DOI: 10.1063/1.2198940
[20] A.K. Tagantsev, G. Gerra. J. Appl. Phys., **100**, 051607 (2006). DOI: 10.1063/1.2337009
[21] A.K. Tagantsev, A.S. Yurkov. J. Appl. Phys., **112**, 044103 (2012). DOI: 10.1063/1.4745037
[22] J. Wawra, K. Nielsch, R. Hühne. Materials, **16**, 6036 (2023). DOI: 10.3390/ma16176036
[23] M. Saghayezhian, Z. Wang, D. Howe, P. Siwakoti, E.W. Plummer, Y. Zhu, J. Zhang. J. Phys.: Condens. Matter., **33**, 275003 (2021). DOI: 10.1088/1361-648X/abfdf1
[24] V. Nagarajan, C.L. Jia, H. Kohlstedt, R. Waser, I.B. Misirlioglu, S.P. Alpay, R. Ramesh. Appl. Phys. Lett., **86**, 192910 (2005). DOI: 10.1063/1.1922579
[25] Biya Cai, J. Schwarzkopf, C. Feldt. Phys. Rev. B, **95**, 184108 (2017). DOI: 10.1103/PhysRevB.95.184108
[26] J. Schwarzkopf, E. Hollmann, D. Braun, M. Schmidbauer, T. Grellmann, R. Wördenweber. Phys. Rev. B, **93**, 224107 (2016). DOI: 10.1103/PhysRevB.93.224107
[27] J. Koruza, P. Groszewic, H. Breitzke, G. Buntkowsky, T. Rojac, B. Malič. Acta Mater., **126**, 77 (2017). DOI: 10.1016/j.actamat.2016.12.049
[28] G. Damamme, C. Guerret-Piécourt, T. Temga, D. Juvé, D. Tréheux. J. Phys. D: Appl. Phys., **41** (6), 065208 (2008). DOI: 10.1088/0022-3727/41/6/065208
[29] *The Materials Project*. Electronic source. Available at: https://materialsproject.org/materials/mp-4681/
[30] *The Materials Project*. Electronic source. Available at: https://materialsproject.org/materials/mp-3671/
[31] C. Villeneuve-Faure, K. Makasheva, L. Boudou, G. Teyssedre. *Space Charge at Nanoscale: Probing Injection and Dynamic Phenomena Under Dark/Light Configurations by Using KPFM and C-AFM*. In U. Celano (ed.). *Electrical Atomic Force Microscopy for Nanoelectronics* (Springer, 2019), p. 267–301. DOI: 10.1007/978-3-030-15612-1_9

Translated by T.Zorina